Adsorption of Crystal Violet with Magnetic Graphene Oxide Nano Adsorbent Synthesized from *Schima wallichii* Wood

Danar Arifka Rahman[1*], Mindriany Syafila[2], and Qomarudin Helmy[2]

[1]*Study Program of Environmental Engineering, Department of Biology, Faculty of Science and Technology, Universitas Airlangga, Kampus C Mulyorejo, Surabaya 60115, Indonesia*

[2]*Water and Wastewater Engineering Expertise Group, Bandung Institute of Technology, Jl. Ganesha No. 10, Bandung 40132, West Java, Indonesia*

* ***Corresponding author:***

email: danar.arifka@fst.unair.ac.id

Received: January 3, 2023
Accepted: August 22, 2023

DOI: 10.22146/ijc.80894

Abstract: *The textile industry continues to experience production developments to reach a target for the country's economic development. The increase in production leads to an increase in the amount of waste generated. Dyes such as crystal violet (CV) in textile wastewater are toxic and difficult to remove by conventional treatment. Adsorption with nano adsorbent has been widely researched and developed to remove dyes in the environment because it has various advantages. Magnetic graphene oxide (GO-Fe_3O_4) as a006E adsorbent has been widely studied because it has a large surface area, strong chemical bonds and is easily separated from the aqueous phase. Puspa (*Schima wallichii*) wood has the potential to be used as a natural source of graphite. The characterization of the adsorbent was tested with FTIR, SEM-EDS, and BET. The equilibrium time for the adsorption process was 20 min, while the optimum adsorbent dose was 0.04 g. Adsorption isotherm and kinetics analysis showed that CV adsorption using MGO followed Langmuir and pseudo-second-order models, respectively. Thermodynamic studies displayed that the CV adsorption was endothermic and spontaneous. The results of this study suggested that the adsorption of CV using GO-Fe_3O_4 nano adsorbent from* S. wallichii *wood proceeds by chemisorption and physisorption.*

Keywords: *adsorption; crystal violet; dyes; nano adsorbent; wastewater*

■ INTRODUCTION

The textile industry is a labor-intensive industry that is a large source of employment and one of the oldest industries in Indonesia. The Indonesian authorities' objective is to increase the cost of national textile and garment exports to USD 75 billion by 2030. Although the textile sector is a rapidly growing sector in the economy, the main problem is the facet outcomes of the industry. Textile production processes are portrayed by long process cycles that generate large amounts of waste and consume large amounts of resources such as water, fuel, and various chemicals. The major environmental issues related to the textile enterprise are usually related to the pollution of water bodies caused by the disposal of untreated sewage [1].

Organic compounds, hazardous chemicals, detergents, and dyes are all present in the wastewater generated by the textile industry. Therefore, the textile enterprise is one of the biggest polluting industrial wastes. Dyes are poisonous to microorganisms and relatively resistant to light and heat. Dyes cannot be effortlessly eliminated through regular treatment because of their complicated structure and artificial origin. Crystal violet (CV) is one of the most widely used dyes in the textile industry. The presence of this substance in water can cause many types of diseases, such as skin, eye and respiratory system irritation and CV is also toxic to the reproductive and nervous systems [2]. Therefore, treatment is needed to degrade CV pollutants in wastewater before being discharged into water bodies.

The most common techniques used for removing dye-containing wastewater are chemical precipitation using lime/ferrous sulfate-based coagulant and ozone/peroxide/Fenton/UV-based advanced oxidation processes (AOPs) [3-4], using the physical and biological treatment and or a combination thereof [5]. Treatment combinations of ozone-based AOPs applied both as pre-treatment and as post-treatment of activated sludge systems are reported to show high performance in removing dyes from textile wastewater [6-7]. Among these methods, adsorption is the most broadly used technique for dye removal due to its great efficiency, simple design, easy handling, and comparatively low cost [8].

Currently, the development of adsorbents based on nanostructured materials is more attractive than conventional sorbents due to their high surface area, excellent mechanical and thermal strength, extensive amount of active sites, and low diffusion resistance within the particles [9]. Graphene oxide (GO) nanomaterial, which is the result of the synthesis of graphite, is one of the carbon-based nanomaterials. GO has several advantages, including its large surface area and strong chemical bonds [10]. However, the separation of GO from water samples is difficult. So, it must be functionalized or combined with other materials. This affects the low recyclability value of the sorbent and GO residues can become secondary contaminants if they cannot be completely separated [11]. One of the nano-particle composites that have been used and can be easily separated from the sample water by an external magnetic field without long centrifugation or filtration is iron oxide (Fe_3O_4) magnetic nanoparticles to form GO-Fe_3O_4 [12].

Previous studies have reported that the synthesis of GO-Fe_3O_4 still uses fabricated graphite as a source substance, but the use of graphite from natural sources is still very little developed [8]. One of the natural sources that have the potential as a source of adsorbent material is Puspa wood (*Schima wallichii*). Puspa is a plant that is widely spread in Indonesia and used as a construction material. There was already a report that researched Puspa seeds into activated carbon [13], but there has been no research that uses Puspa wood as a source of biomass.

In this study, the synthesis of GO-Fe_3O_4 nanomaterial from Puspa wood as a source of natural graphite for dye adsorption was carried out. The optimization parameters to be studied were contact time and adsorbent dose. In addition, the characteristics, isotherms, kinetics, thermodynamics, and reusability will also be displayed.

■ EXPERIMENTAL SECTION

Materials

The materials used in this research were 80% sodium hydroxide (NaOH, Merck Millipore; for analysis), sodium nitrate ($NaNO_3$, Merck Millipore; for analysis), potassium permanganate ($KMnO_4$, Merck Millipore; for analysis), 37% hydrogen peroxide (H_2O_2, Merck Smart Lab; analytical reagent) solution, 97% sulfuric acid (H_2SO_4, Merck Smart Lab; analytical reagent) solution, 5% hydrogen chloride (HCl, Merck Millipore; for analysis) solution, iron(III) chloride hexahydrate ($FeCl_3{\cdot}6H_2O$, Meck Schuchardt; anhydrous for synthesis) and iron(II) sulfate heptahydrate ($FeSO_4{\cdot}7H_2O$, Merck Millipore; for analysis) which obtained from the Water Quality Laboratory, Bandung Institute of Technology. Puspa wood (*Schima wallichii*) sample (Fig. 1) was taken from Bandung City, West Java, Indonesia.

Procedure

Preparation of graphene oxide-magnetic nano adsorbent

The Puspa wood was cut into small pieces, washed with distilled water and dried in an oven at 105 °C for 24 h

Fig 1. *Schima wallichii* sample and pyrolysis process preparation

to reduce the moisture content. Afterward, Puspa wood went through a pyrolysis process at 400 °C for 30 min in a furnace. The carbon products were then pulverized with a high-energy ball mill to reduce the graphite to nano size [8,14].

The synthesis of GO was done using Hummer's method with modification [10]. A 5 g of carbon nano size was added in 95% H_2SO_4 (115 mL) and $NaNO_3$ (2.5 g). In addition, the mixture was set in an ice bath (< 10 °C) while stirring for 1 h. Afterward, 15 g of $KMnO_4$ was gradually added over 2 h, and the temperature was kept under control below 10 °C. Then the temperature of the suspension was raised to 35 °C for half an hour while still stirring, then 230 mL of distilled water was added and left for 15 min. Finally, 700 mL of distilled water and 10 mL of 37% H_2O_2 were added to terminate the oxidation. The mixture was then centrifuged and rinsed several times with 5% HCl solution and distilled water and then followed by drying for 24 h in the oven at 105 °C.

The procedure for making magnetic graphene oxide (MGO) was using the co-precipitation procedure [8]. A 0.6 g of GO was sonicated in 50 mL of deionized water over 15 min. A 100 mL solution containing $FeSO_4{\cdot}7H_2O$ (0.656 g) and $FeCl_3{\cdot}6H_2O$ (1.181 g) was mixed continuously for 30 min at 40 °C. The dispersed GO solution was then put into the Fe(II)/Fe(III) mixture and mixed for 30 min. The solution was adjusted to pH 10 with 50% NaOH and left for 30 min. The product was then separated magnetically, cleaned with deionized water, and dried at 105 °C for 24 h. MGO nano adsorbents that have been made are characterized to determine the characteristics of the adsorbents made. The characterization tests used were scanning electron microscope–energy dispersive X-ray spectroscopy (SEM-EDS), Fourier transform infrared (FTIR), and Brunauer, Emmet, and Teller (BET) [3,8,15].

Adsorption experiment

The experiment of this research was carried out by batch adsorption method. The variables used were contact time and adsorbent dose. The independent variables used were contact time of 0–120 min and adsorbents dose of 10–50 mg. Measurement of CV concentrations after each experiment was carried out with a UV-vis spectrophotometer at a wavelength of 580 nm. The adsorption capacity and removal percentage were calculated using Eq. (1) and (2);

$$Q_e = \frac{(C_o - C_e)V}{m} \quad (1)$$

$$R(\%) = \frac{C_o - C_e}{C_o} \times 100 \quad (2)$$

where Q_e is adsorption capacity (mg/g), C_o is CV initial concentration (mg/L), C_e is CV equilibrium concentration (mg/L), V is solution volume (L), and m is adsorbent dose (mg). The isotherms model used were the Freundlich and Langmuir isotherms. The kinetic models used were pseudo-first-order (PFO) and pseudo-second-order (PSO) models. The thermodynamic adsorption parameters were calculated at different temperatures (298, 303, 313 and 323 K). OriginPro 2022b and Microsoft Excel were used to analyze the adsorption isotherms, kinetics, and thermodynamics.

■ RESULTS AND DISCUSSION

SEM-EDS Characterization

SEM-EDS testing on GO and GO-Fe_3O_4 nano adsorbents was carried out to determine the surface morphology of the adsorbents and the elements that compose them. The test results for the GO and MGO samples are presented in Fig. 2. The surface morphology of the adsorbent appears to have a fairly high level of ripple so that the surface area becomes larger. This surface area is very useful for CV attachment media, which can improve its adsorption performance. GO adsorbents have several main elements, namely carbon (C) and oxygen (O), with a ratio of % C:O atoms of 66.97:32.15. This confirms the success of the graphite oxidation process in the presence of oxygenated functional groups in GO. Meanwhile, EDS testing on the MGO sample showed that there were magnetic nanoparticle elements in GO with several dominant elements, namely carbon (C), oxygen (O), and iron (Fe), with a % atom ratio of 41.14:41.11:16.32.

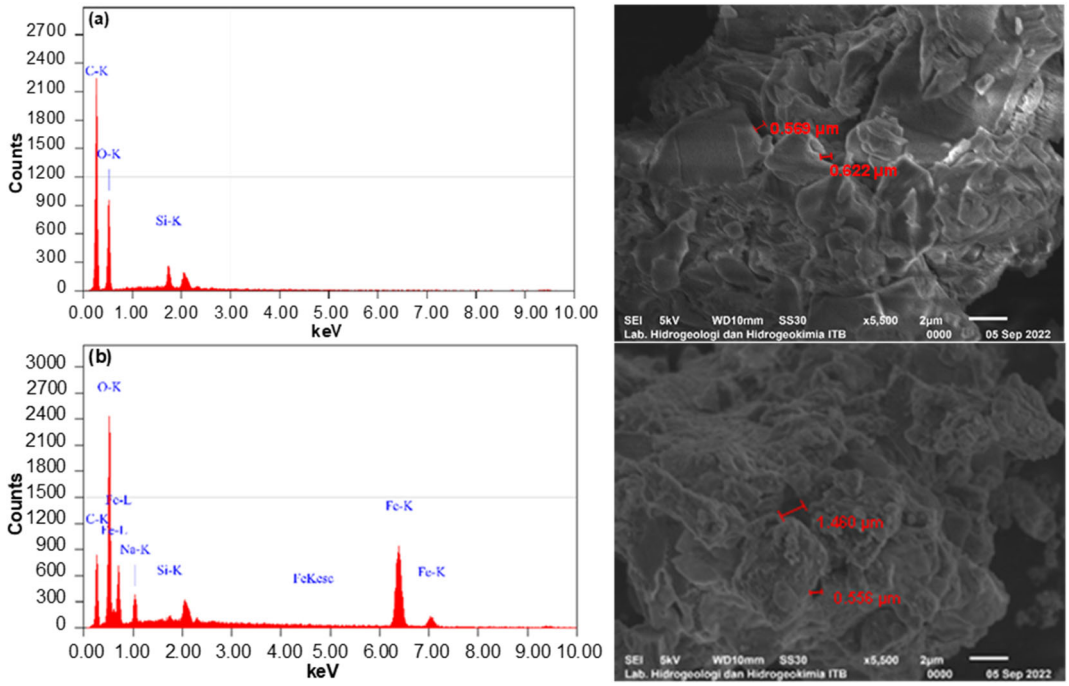

Fig 2. SEM-EDS data of (a) GO and (b) MGO

FTIR Characterization

The test of GO and GO-Fe_3O_4 adsorbents using FTIR is to identify what functional groups are present in the adsorbent material. The characterization of the adsorbent before the adsorption process using FTIR was observed with a wavelength of 500–4000 cm^{-1} where in the range of wavenumbers it can be seen the characteristics of the vibrational absorption of functional groups possessed by GO and GO-Fe_3O_4 materials. Each chemical functional group has its frequency [8]. The absorbance peak value in the 2000–4000 cm^{-1} spectrum, as shown in Fig. 3, looks lower than the 500–2000 cm^{-1} spectrum peak. This explains that the functional groups in the spectrum are relatively few compared to other spectra.

Based on the FTIR spectrum of GO, information was obtained on the presence of stretching vibrations of the hydroxyl (–OH) functional group shown by the wave peak at 3217.46 cm^{-1}. The wide peak in this region is a characteristic of –OH that undergoes the formation of hydrogen bonds. The vibration peak at 2011.17 cm^{-1} was the property of the carbonyl or carboxyl group. Moreover, the C=C aromatic characteristic of Puspa wood, which was not completely oxidized, is indicated by wavenumber 1556.24 cm^{-1}. The peaks of 1373.03 and 1111.60 cm^{-1}

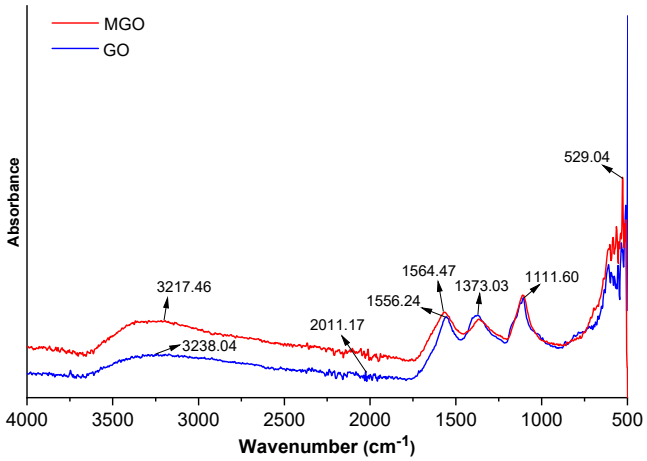

Fig 3. FTIR test results

belong to the C–O–C (epoxy) and C–O (alkoxy) strain vibrations, respectively [16]. These results prove that natural graphite from Puspa wood was effectively oxidized to GO, as indicated by the existence of plentiful oxygen-containing functional groups on the adsorbent structure.

In the spectrum of the MGO nano adsorbent, it is seen that there is a peak at 3238.04 cm^{-1}, which shows the characteristics of –OH group. The width of the peak in this vibrational region is a feature of –OH group that undergoes hydrogen bonding. Vibration at 1564.47 cm^{-1}

indicates stretching vibration properties of the C=C group. FTIR analysis can also provide strong clues about the formation of C–O–Fe coordination bonds between GO and Fe_3O_4. This is evident from the Fe–O stretching vibrations on Fe_3O_4 nanoparticles at 529.04 cm^{-1}, confirming the successful loading of Fe_3O_4 on the GO surface. Fe(II) and Fe(III) on Fe_3O_4 nanoparticles interacted in coordination chemical bonds with carbonyl and –OH groups on the GO surface [17].

BET Characterization

BET analysis was used to identify the surface characteristics of the adsorbent related to the surface area, pore volume, and pore diameter. The BET test results for GO and MGO are shown in Table 1. Based on the test results, the specific surface area of GO and MGO were 3.7806 and 12.8831 m^2/g, respectively. The area of the adsorbent is related to the physical strength of the adsorbent material, where the larger the area, the more micropores there will be, thereby inhibiting the adsorption of large molecules. Theoretically, the specific surface area of the GO monolayer should be slightly below 2,630 m^2/g, but the specific surface area of GO, according to the literature, is often much smaller. Esmaeili et al. [18] mentioned that in practice, the specific surface area of GO is in the range of 2 to 1,000 m^2/g. This is much smaller than the theory, primarily due to the drying process that causes particle stacking. As known, GO can be exfoliated perfectly and dispersed evenly in water. Thus, measuring the surface area directly in water can prevent GO from agglomerating [19].

The average pore diameters of GO and MGO adsorbents were 4.2782 and 3.1518 nm, which, based on the classification of pore types by IUPAC, were in the mesopore (2–50 nm) group. The larger pore diameter of GO than MGO can be attributed to the addition of Fe in the GO structure, which reduces the pore size of the adsorbent [20]. The size of the diameter of the adsorbent then needs to be compared with the diameter of CV to determine the size comparison. According to Cotoruelo et al. [21], the diameter of CV molecule is 1.4 nm. Based on the comparison of the pore diameter of the adsorbent and the size of the molecule, it can be seen that CV molecules can enter the pores of MGO nano adsorbents.

Effect of Contact Time

Contact time is a very influential variable because it determines how long the adsorption process takes. The contact time variable was also used to determine the equilibrium time of the adsorption and to understand the adsorption kinetics. The contact time variable test is also used to improve processing quality and find ways to save processing costs. The % removal and adsorption capacity of MGO nano adsorbent is illustrated in Fig. 4.

The test for the contact time variable was carried out with an adsorbent mass of 0.0206 g, initial pH 4.91 and initial CV concentration of 50 mg/L (300 mL). The initial pH value was obtained from distilled water available in the laboratory. The entire series of studies used the same average pH value of distilled water.

Table 1. BET test results

Characteristics	Unit	GO	MGO
Specific surface area	m^2/g	3.7806	12.8831
Total pore volume	cc/g	0.0099	0.0244
Average pore diameter	nm	4.2782	3.1518

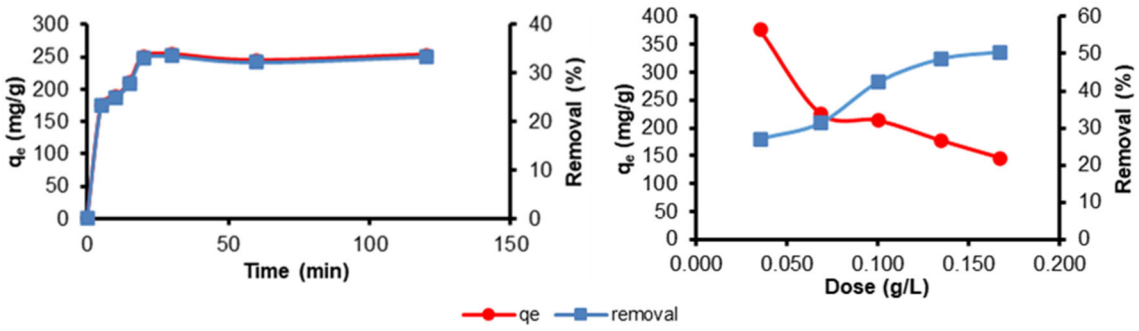

Fig 4. Effect of contact time and adsorbent dose on CV adsorption

The adsorption reaction was conditioned at room temperature (26 ± 1 °C) with 120 rpm stirring. The adsorption process was carried out by varying the contact time from 5 to 120 min to determine the adsorption equilibrium time. Separation of adsorbent and adsorbate was carried out using an external magnet for each sampling. The adsorbate that has been separated from the adsorbent is measured using a UV-vis spectrophotometer at a wavelength of 580 nm and calculated by the calibration curve that has been made.

results showed that CV was adsorbed on the MGO surfaces linearly over a contact time of 5–20 min. The graph of the effect of contact time shows a slight decrease in the concentration of adsorbates adsorbed on the adsorbent. This is due to the monolayer GO structure so that the bound adsorbate is more easily separated than the multilayer adsorbent structure [22]. Based on these results, the equilibrium time for both adsorbents is 20 min.

Effect of Adsorbent Dose

The adsorbent dose is a significant factor affecting the adsorption process. The mass of GO and GO-Fe_3O_4 adsorbent in the range of 10–50 mg was used to remove CV, as shown in Fig. 4. This parameter test used a 300 mL CV solution (50 mg/L) at room temperature (25 ± 1 °C) and 20 min of equilibrium time. The adsorption process used stirring at 120 rpm. The % removal and adsorption capacity of MGO nano adsorbent is illustrated in Fig. 4.

The efficiency of CV removal increased with increasing the dose of adsorbent used, whereas in GO adsorbent, the efficiency increased from 33.63 ± 0.82% at 10 mg to 83.58 ± 0.11% at 50 mg adsorbent. Meanwhile, the removal efficiency with MGO adsorbent increased from 27.03 ± 0.22 to 50.44 ± 0.48%. These results are inversely proportional to the observations on adsorption capacity. In the adsorption process with 10 mg GO adsorbent, the adsorption capacity obtained was 517.07 ± 35 mg/g. Meanwhile, the capacity of adsorption at 50 mg adsorbent dose was 264.26 ± 3.66 mg/g. In the adsorption process using GO-Fe_3O_4 adsorbent, the adsorption capacity obtained decreased from 375.89 ± 6.2 mg/g at a dose of 10 mg to 145.73 ± 1.62 mg/g at a dose of 50 mg.

This phenomenon can be explained by the fact that the addition of the adsorbent mass will enhance the surface area, thereby increasing the number of adsorption sites that exist; this is similar to other studies [23-24]. The increase in surface area and adsorption sites will increase the efficiency of CV removal. However, the quantity of unsaturated adsorption sites will rise, thereby reducing the capacity of adsorption. This is because the more adsorbents used will also increase the possibility of aggregation between adsorbent particles [25].

Adsorption Isotherm

The adsorption isotherm is used to analyze the interactions between the adsorbate and the adsorbent. This is also related to the adsorption mechanism that occurs. Based on Ciğeroğlu et al. [26] research, the process of adsorption of dye to the surface of the GO adsorbent occurs physically. Meanwhile, according to Shoushtarian et al. [25], the adsorption of dye onto the surface of the GO adsorbent occurs chemically. Fig. 5 shows the Langmuir and Freundlich nonlinear isotherm models for the adsorption of CV using MGO nano adsorbent. Based on the experimental results, the interactions that occur between the adsorbate and the adsorbent using the Langmuir and Freundlich isotherms, whose parameter values are shown in Table 2.

Isotherm analysis was carried out at equilibrium time, specifically after 20 min of the adsorption process. The Langmuir isotherm assumes the adsorption of the adsorbate monolayer onto the adsorbent surface with a limited range of similar sites and the same energy sites. The Freundlich isotherm assumes that the adsorbent surface is heterogeneous, so the adsorption occurs in a multilayer. This isotherm model also defines the exponential distribution of the active surface of the

Table 2. Adsorption isotherms parameters

Langmuir		Freundlich	
Q_m (mg/g)	221.2940	1/n	0.2812
K_L (L/mg)	0.2218	K_F	69.0633
R^2	0.9658	R^2	0.9489

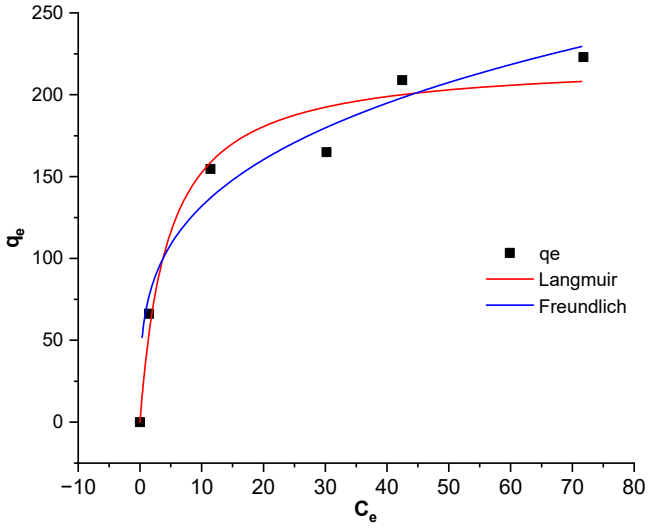

Fig 5. Plots of Langmuir and Freundlich isotherm models for the adsorption of CV into MGO nano adsorbent

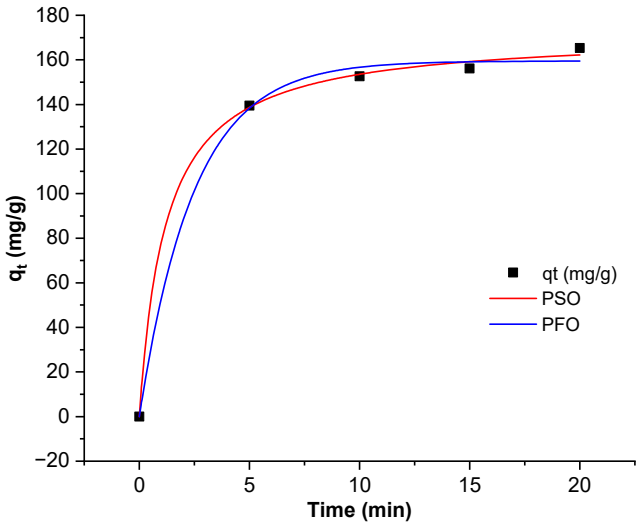

Fig 6. Plots of PFO and PSO nonlinear models for the adsorption of CV into MGO nano adsorbent

adsorbent [27-29]. Adsorption isotherm analysis with the Freundlich model to analyze the assumption that the adsorption process is not limited to one layer or chemisorption.

The correlation coefficient (R^2) of the Langmuir isotherm model is higher than the Freundlich isotherm. Therefore, the Langmuir model is better at describing the adsorption process of CV dye on MGO nano adsorbent. This indicates that the CV dye was adsorbed on the MGO monolayer surface with a maximum adsorption capacity of 221.2940 mg/g. The 1/n value, which is smaller than 1, equal to 0.2812, indicates the possible conditions during adsorption [3,30].

Adsorption Kinetics

Adsorption kinetics was studied to identify the adsorption mechanism in the adsorption process by studying the relationship between adsorption capacity and contact time. Adsorption kinetics is influenced by several factors, such as diffusion rate, mass transfer, adsorption rate and dynamic equilibrium [31]. Fig. 6 shows the pseudo-first-order (PFO) and pseudo-second-order (PSO) nonlinear plots. The various kinetics parameters were calculated, as shown in Table 3.

The value of the determination coefficient (R^2) of the PSO is known to be higher than PFO. Furthermore, the value of the adsorption capacity calculated by the PSO

Table 3. Adsorption kinetics parameters

PFO		PSO	
Q_e (mg/g)	159.4960	Q_e (mg/g)	171.9390
K_1 (1/min)	0.1040	K_2 (1/mg min)	0.0048
R^2	0.9968	R^2	0.9989

kinetic model is closer to the value of the adsorption capacity of the experimental results. These findings stated that the adsorption of CV cationic dye follows PSO kinetic model. This result is also in accordance with several previous studies that reported the suitability of PSO kinetics with the adsorption of cationic dyes on GO-based nano adsorbents [32].

Adsorption Thermodynamics

The thermodynamic parameters of CV dye pollutant adsorption on the surface of MGO nano adsorbent include Gibbs free energy changes (ΔG°), enthalpy (ΔH°), and entropy (ΔS°) were identified in different temperatures (298, 303, 313 and 323 K). The internal energy and orientation changes occurring during the adsorption of CV dye with MGO nano adsorbent were studied using equilibrium time. The thermodynamic plotting and parameter values are shown in Fig. 7 and Table 4, respectively. ΔG° is the energy required for the reaction process, in this case, the adsorption process. The value of ΔG° on MGO nano

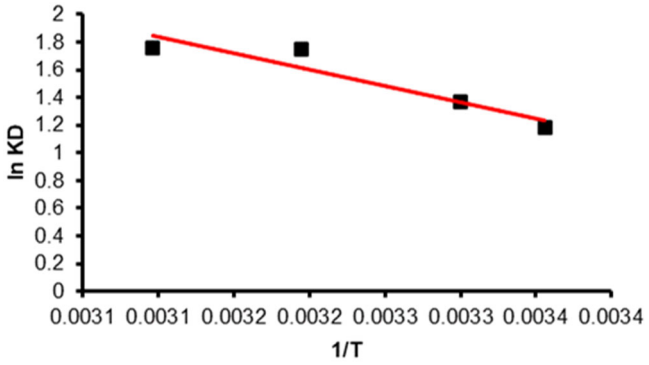

Fig 7. Thermodynamic plot of CV removal

Table 4. Thermodynamic parameters of CV removal

Temperature (K)	ΔG°	ΔS°	ΔH°
298	−3.0630	0.0758	19.5096
303	−3.4420		
313	−4.1990		
323	−4.9560		

adsorbent was in the range of −20 to 0 kJ/mol, which indicates that the adsorption process that occurs is physical adsorption [33]. It also suggests that the adsorption process takes place spontaneously. The ΔS° value close to 0 indicates low irregularity on the surface of the MGO nano adsorbent during the adsorption process. Meanwhile, a positive ΔH° value indicates that the adsorption process that occurs is an endothermic process.

■ CONCLUSION

Magnetic graphene oxide (MGO) nano adsorbent has been successfully synthesized from Puspa wood (*Schima wallichii*). The optimum conditions for crystal violet (CV) dye adsorption using MGO nano adsorbent could be received at 0.04 g adsorbent dose and a contact time of 20 min. Adsorption kinetics analysis showed that CV dye adsorption using MGO followed a pseudo-second-order. Meanwhile, according to the adsorption isotherm, CV dye adsorption using MGO follows the Langmuir isotherm model. Therefore, it can be assumed that CV adsorption using MGO occurred through chemisorption. Furthermore, based on thermodynamic studies, it can be discovered that the CV adsorption process using MGO nano adsorbent was controlled not only by chemisorption but also by physisorption. The adsorption process takes place spontaneously and endothermic. The use of non-fabricated materials as a source of graphite to synthesize MGO has good prospects in the future.

■ ACKNOWLEDGMENTS

The authors are grateful for the providing of materials and laboratory facilities from the Bandung Institute of Technology as part of this research.

■ AUTHOR CONTRIBUTIONS

Danar Arifka Rahman, who is also the corresponding author, acted as investigator, conducted calculations, and wrote the manuscript. Mindriany Syafila and Qomarudin Helmy wrote, made revisions and final assessments of the data and reports.

■ REFERENCES

[1] Suryawan, I.W.K., Helmy, Q., and Notodarmojo, S., 2018, Textile wastewater treatment: Colour and COD removal of reactive black-5 by ozonation, *IOP Conf. Ser.: Earth Environ. Sci.*, 106 (1), 012102.

[2] Munagapati, V.S., and Kim, D.S., 2016, Adsorption of anionic azo dye Congo Red from aqueous solution by cationic modified orange peel powder, *J. Mol. Liq.*, 220, 540–548.

[3] Sh. Gohr, M., Abd-Elhamid, A.I., El-Shanshory, A.A., and Soliman, H.M.A., 2022, Adsorption of cationic dyes onto chemically modified activated carbon: Kinetics and thermodynamic study, *J. Mol. Liq.*, 346, 118227.

[4] Helmy, Q., Suryawan, I.W.K., and Notodarmojo, S., 2022, "Ozone-Based Processes in Dye Removal" in *Advanced Oxidation Processes in Dye-Containing Wastewater: Volume 2*, Eds. Muthu, S.S., and Khadir, A., Springer Nature Singapore, Singapore, 175–211.

[5] Pratiwi, R., Notodarmojo, S., and Helmy, Q., 2018, Decolourization of remazol black-5 textile dyes using moving bed bio-film reactor, *IOP Conf. Ser.: Earth Environ. Sci.*, 106 (1), 012089.

[6] Suryawan, I.W.K., Helmy, Q., and Notodarmojo, S., 2020, Laboratory scale ozone-based post-treatment from textile wastewater treatment plant effluent for water reuse, *J. Phys.: Conf. Ser.*, 1456 (1), 012002.

[7] Suryawan, I.W.K., Septiariva, I.Y., Helmy, Q., Notodarmojo, S., Wulandari, M., Sari, N.K., Sarwono, A., Pratiwi, R., and Lim, J.W., 2021, Comparison of ozone pre-treatment and post-treatment hybrid with moving bed biofilm reactor in removal of remazol black 5, *Int. J. Technol.*, 12 (4), 727–738.

[8] Neolaka, Y.A.B., Lawa, Y., Naat, J.N., Riwu, A.A.P., Iqbal, M., Darmokoesoemo, H., and Kusuma, H.S., 2020, The adsorption of Cr(VI) from water samples using graphene oxide-magnetic (GO-Fe_3O_4) synthesized from natural cellulose-based graphite (Kusambi wood or *Schleichera oleosa*): Study of kinetics, isotherms and thermodynamics, *J. Mater. Res. Technol.*, 9 (3), 6544–6556.

[9] Liu, S., Ma, C., Ma, M.G., and Xu, F., 2019, "Magnetic Nanocomposite Adsorbents" in *Composite Nanoadsorbents*, Eds. Kyzas, G.Z., and Mitropoulos, A.C., Elsevier, Amsterdam, Netherlands 295–316.

[10] Supriyanto, G., Rukman, N.K., Khoiron Nisa, A., Jannatin, M., Piere, B., Abdullah, A., Zakki Fahmi, M., and Septya Kusuma, H., 2018, Graphene oxide from Indonesian biomass: Synthesis and characterization, *BioResources*, 13 (3), 4832–4840.

[11] Wang, H., Yuan, X., Wu, Y., Chen, X., Leng, L., Wang, H., Li, H., and Zeng, G., 2015, Facile synthesis of polypyrrole decorated reduced graphene oxide–Fe_3O_4 magnetic composites and its application for the Cr(VI) removal, *Chem. Eng. J.*, 262, 597–606.

[12] Bagheri, A.R., Ghaedi, M., Asfaram, A., Bazrafshan, A.A., and Jannesar, R., 2017, Comparative study on ultrasonic assisted adsorption of dyes from single system onto Fe_3O_4 magnetite nanoparticles loaded on activated carbon: Experimental design methodology, *Ultrason. Sonochem.*, 34, 294–304.

[13] Bhomick, P.C., Supong, A., Karmaker, R., Baruah, M., Pongener, C., and Sinha, D., 2019, Activated carbon synthesized from biomass material using single-step KOH activation for adsorption of fluoride: Experimental and theoretical investigation, *Korean J. Chem. Eng.*, 36 (4), 551–562.

[14] Alam, S., Khan, M.S., Bibi, W., Zekker, I., Burlakovs, J., Ghangrekar, M.M., Bhowmick, G.D., Kallistova, A., Pimenov, N., and Zahoor, M., 2021, Preparation of activated carbon from the wood of *Paulownia tomentosa* as an efficient adsorbent for the removal of acid red 4 and methylene blue present in wastewater, *Water*, 13 (11), 1453.

[15] Moges, A., Nkambule, T.T.I., and Fito, J., 2022, The application of GO-Fe_3O_4 nanocomposite for chromium adsorption from tannery industry wastewater, *J. Environ. Manage.*, 305, 114369.

[16] Cheruiyot, G.K., Wanyonyi, W.C., Kiplimo, J.J., and Maina, E.N., 2019, Adsorption of toxic crystal violet dye using coffee husks: Equilibrium, kinetics and thermodynamics study, *Sci. Afr.*, 5, e00116.

[17] Sammaiah, A., Huang, W., and Wang, X., 2018, Synthesis of magnetic Fe_3O_4/graphene oxide nanocomposites and their tribological properties under magnetic field, *Mater. Res. Express*, 5 (10), 105006.

[18] Esmaeili, A., and Entezari, M.H., 2014, Facile and fast synthesis of graphene oxide nanosheets via bath ultrasonic irradiation, *J. Colloid Interface Sci.*, 432, 19–25.

[19] Zhang, S., Wang, H., Liu, J., and Bao, C., 2020, Measuring the specific surface area of monolayer graphene oxide in water, *Mater. Lett.*, 261, 127098.

[20] Li, S., 2019, Combustion synthesis of porous MgO and its adsorption properties, *Int. J. Ind. Chem.*, 10 (1), 89–96.

[21] Cotoruelo, L.M., Marqués, M.D., Díaz, F.J., Rodríguez-Mirasol, J., Rodríguez, J.J., and Cordero, T., 2012, Lignin-based activated carbons as adsorbents for crystal violet removal from aqueous solutions, *Environ. Prog. Sustainable Energy*, 31 (3), 386–396.

[22] Othman, N.H., Alias, N.H., Shahruddin, M.Z., Abu Bakar, N.F., Nik Him, N.R., and Lau, W.J., 2018, Adsorption kinetics of methylene blue dyes onto magnetic graphene oxide, *J. Environ. Chem. Eng.*, 6 (2), 2803–2811.

[23] Mahmoud, M.A., 2020, Oil spill cleanup by raw flax fiber: Modification effect, sorption isotherm, kinetics and thermodynamics, *Arabian J. Chem.*, 13 (6), 5553–5563.

[24] Chen, F., Liang, W., Qin, X., Jiang, L., Zhang, Y., Fang, S., and Luo, D., 2021, Preparation and recycled simultaneous adsorption of methylene blue and Cu^{2+} co-pollutants over carbon layer encapsulated Fe_3O_4/graphene oxide nanocomposites rich in amino and thiol groups, *Colloids Surf., A*, 625, 126913.

[25] Shoushtarian, F., Moghaddam, M.R.A., and Kowsari, E., 2020, Efficient regeneration/reuse of graphene oxide as a nanoadsorbent for removing basic Red 46 from aqueous solutions, *J. Mol. Liq.*, 312, 113386.

[26] Ciğeroğlu, Z., Haşimoğlu, A., and Özdemir, O.K., 2021, Synthesis, characterization and an application of graphene oxide nanopowder: methylene blue adsorption and comparison between experimental data and literature data, *J. Dispersion Sci. Technol.*, 42 (5), 771–783.

[27] Bonilla-Petriciolet, A., Mendoza-Castillo, D.I., and Reynel-Ávila, H.E., 2017, *Adsorption Processes for Water Treatment and Purification*, Springer Cham, Switzerland.

[28] Ragadhita, R., and Nandiyanto, A.B.D., 2021, How to calculate adsorption isotherms of particles using two-parameter monolayer adsorption models and equations, *Indones. J. Sci. Technol.*, 6 (1), 205–234.

[29] Mozaffari Majd, M., Kordzadeh-Kermani, V., Ghalandari, V., Askari, A., and Sillanpää, M., 2022, Adsorption isotherm models: A comprehensive and systematic review (2010–2020), *Sci. Total Environ.*, 812, 151334.

[30] Alrobei, H., Prashanth, M.K., Manjunatha, C.R., Kumar, C.B.P., Chitrabanu, C.P., Shivaramu, P.D., Kumar, K.Y., and Raghu, M.S., 2021, Adsorption of anionic dye on eco-friendly synthesised reduced graphene oxide anchored with lanthanum aluminate: Isotherms, kinetics and statistical error analysis, *Ceram. Int.*, 47 (7, Part B), 10322–10331.

[31] Oprea, A., Degler, D., Barsan, N., Hemeryck, A., and Rebholz, J., 2019, "Basics of Semiconducting Metal Oxide–based Gas Sensors" in *Gas Sensors Based on Conducting Metal Oxides*, Eds. Barsan, N., and Schierbaum, K., Elsevier, Amsterdam, Netherlands, 61–165.

[32] Rahman, D.A., Helmy, Q., Syafila, M., and Gumilar, A., 2022, Adsorption of dyes using graphene oxide-based nano-adsorbent: A review, *Jurnal Presipitasi*, 19 (2), 384–397.

[33] Faghihi, A., Vakili, M.H., Hosseinzadeh, G., Farhadian, M., and Jafari, Z., 2016, Synthesis and application of recyclable magnetic freeze-dried graphene oxide nanocomposite as a high capacity adsorbent for cationic dye adsorption, *Desalin. Water Treat.*, 57 (47), 22655–22670.